

## Correlated Electron State in $\text{Ce}_{1-x}\text{Yb}_x\text{CoIn}_5$ Stabilized by Cooperative Valence Fluctuations

L. Shu,<sup>1</sup> R. E. Baumbach,<sup>1</sup> M. Janoschek,<sup>1</sup> E. Gonzales,<sup>1</sup> K. Huang,<sup>1</sup> T. A. Sayles,<sup>1</sup> J. Paglione,<sup>2</sup> J. O'Brien,<sup>3</sup> J. J. Hamlin,<sup>1</sup>  
D. A. Zocco,<sup>1</sup> P.-C. Ho,<sup>4</sup> C. A. McElroy,<sup>1</sup> and M. B. Maple<sup>1,\*</sup>

<sup>1</sup>*Department of Physics, University of California, San Diego, La Jolla, California 92093, USA*

<sup>2</sup>*Center for Nanophysics and Advanced Materials, Department of Physics, University of Maryland, College Park, Maryland 20742, USA*

<sup>3</sup>*Quantum Design, San Diego, California 92121, USA*

<sup>4</sup>*Department of Physics, California State University, Fresno, California 93740, USA*

(Received 23 December 2010; published 13 April 2011)

X-ray diffraction, electrical resistivity, magnetic susceptibility, and specific heat measurements on  $\text{Ce}_{1-x}\text{Yb}_x\text{CoIn}_5$  ( $0 \leq x \leq 1$ ) reveal that many of the characteristic features of the  $x = 0$  correlated electron state are stable for  $x \leq 0.775$  and that phase separation occurs for  $x > 0.775$ . The stability of the correlated electron state is apparently due to cooperative behavior of the Ce and Yb ions, involving their unstable valences. Low-temperature non-Fermi liquid behavior is observed and varies with  $x$ , even though there is no readily identifiable quantum critical point. The superconducting critical temperature  $T_c$  decreases linearly with  $x$  towards 0 K as  $x \rightarrow 1$ , in contrast with other HF superconductors where  $T_c$  scales with  $T_{\text{coh}}$ .

DOI: 10.1103/PhysRevLett.106.156403

PACS numbers: 71.10.Hf, 71.27.+a, 74.70.Tx, 75.30.Mb

One of the important issues in the study of correlated electron physics is the relationship between quantum criticality (QC), non-Fermi-liquid (NFL) behavior, and unconventional superconductivity (SC). It is generally thought that critical fluctuations associated with a magnetic quantum critical point (QCP), where a second-order magnetic phase transition is suppressed to 0 K by an external control parameter [e.g., composition ( $x$ ), pressure ( $P$ ), or magnetic field ( $H$ )], can provide a mechanism for NFL behavior and unconventional SC in a narrow “dome” around the QCP [1] (e.g.,  $\text{CeIn}_3$ ,  $\text{CePd}_2\text{Si}_2$ , and  $\text{CeCu}_{6-x}\text{Au}_x$ ) [2,3]. However, the precise nature of the relationship between these phenomena remains to be understood, particularly since many compounds have been reported where the NFL behavior persists over an extended region of the phase diagram in the absence of any identifiable QCP [4].

Ce-based compounds have been studied extensively within the context of the QCP scenario because the Ce valence is sensitive to applied or chemical pressure, which often allows the magnetic ordering temperature to be tuned towards 0 K. One example is the family of materials  $\text{CeMIn}_5$  ( $M = \text{Co}, \text{Rh}, \text{Ir}$ ). These compounds exhibit a variety of unusual ground states that appear to be strongly influenced by nearness to QCPs or QC regions in the  $T - P - x - H$  phase space. Of these,  $\text{CeCoIn}_5$  has been the focus of much attention. It is believed to be situated near an antiferromagnetic QCP that can be accessed by “negative” pressure [5], as was demonstrated by a combination of studies involving the application of pressure and substitution of Rh for Co [6]. The normal-state electrical resistivity shows NFL-like  $T$ -linear behavior, in accord with the system being near to a 2D antiferromagnetic QCP [5]. Upon application of pressure, the SC transition is suppressed to 0 K, and a FL-like quadratic  $T$  dependence

of the electrical resistivity is restored, as expected for the prototypical QCP scenario. A second magnetic-field-induced QCP is observed upon suppression of the SC state [7,8]. In addition, the  $H - T$  phase diagram is unusual, in that the transition from the normal to the SC phase is first order at high  $H$  [9,10], and there is a second magnetically ordered SC phase that exists only at low  $T$  and high  $H$  close to the upper critical field  $H_{c2}$  [11].

In this Letter, we report results for the series  $\text{Ce}_{1-x}\text{Yb}_x\text{CoIn}_5$  which demonstrate that Yb substitution constitutes a useful tuning parameter for exploring QC phenomena in  $\text{CeCoIn}_5$ . Initially, our study was motivated by the observation that both Cooper pair breaking and Kondo-lattice coherence are uniformly influenced by magnetic and nonmagnetic rare earth ( $R$ ) substituents for  $\text{Ce}_{1-x}R_x\text{CoIn}_5$ . In contrast, the NFL behavior is strongly dependent on the  $f$ -electron configuration of the  $R$  ions [12]. In a simple picture, Yb substitution is expected to yield similar results. However, Yb is distinguished from other  $R$  and lanthanide elements in several ways. For instance, Yb frequently exhibits a valence ( $\nu$ ) instability ( $2+ \leq \nu_{\text{Yb}} \leq 3+$ ), similar to Ce ( $3+ \leq \nu_{\text{Ce}} \leq 4+$ ). Another parallel is found in the electron-hole analogy between  $\text{Ce}^{3+}$  ( $4f^1$ ) and  $\text{Yb}^{3+}$  ( $4f^{13}$ ). However, Ce and Yb also exhibit several significant differences; e.g., applied pressure causes Yb to become more magnetic and Ce to become less magnetic.

Our study reveals that, as Yb is substituted for Ce, many of the exemplary correlated electron effects observed for  $\text{CeCoIn}_5$  are only weakly affected, in marked contrast with what is seen for other  $R$  substitutions in this system. In summary, (1) the lattice parameters remain nearly constant for  $x \leq 0.775$ , after which phase separation into Yb rich and deficient phases of  $\text{Ce}_{1-x}\text{Yb}_x\text{CoIn}_5$  occurs. (2) The SC

transition temperature is weakly suppressed with  $x$  and extends to the phase separation region. The extrapolation of the  $T_c$  vs  $x$  curve for  $x > 0.775$  suggests that, in the absence of phase separation, SC would disappear near  $x = 1$ . This finding is remarkable, as other  $R$  substitutions in  $Ce_{1-x}R_xCoIn_5$  suppress SC at approximately  $x = 0.25$  [12]. (3) The Kondo-like coherence temperature  $T_{coh}$  may be weakly suppressed for low  $x$ , after which it remains roughly constant up to  $x = 0.775$ . These results are particularly striking if we consider that, in contrast to other heavy fermion SCs,  $T_c$  does not scale with  $T_{coh}$  [13], except possibly for small  $x$ . (4) The heavy electron mass and effective magnetic moment remain roughly constant up to  $x = 0.775$ . (5) The NFL behavior is strongly influenced by Yb substitution and persists up to  $x = 0.65$ , after which a recovery of FL-like behavior is observed with increasing  $x$ . Taken together, these properties suggest that, unlike in other  $Ce_{1-x}R_xCoIn_5$  series, the Ce and Yb ions adopt cooperative intermediate valence (IV) states, resulting in the preservation of the coherent Kondo-like lattice and SC, while the associated valence fluctuations (VFs) strongly tune the NFL state [14].

Single crystals of  $Ce_{1-x}Yb_xCoIn_5$  ( $0 \leq x \leq 1$ ) were synthesized by using an indium self-flux method [15]. The crystal structure and chemical composition were verified by means of x-ray powder diffraction (XRD) and energy dispersive x-ray (EDX) analysis (Fig. 1). The lattice parameters  $a$  and  $c$  were determined by means of Rietveld refinement [Fig. 1(a)]. According to Vegard's law, the lattice constants should decrease linearly with increasing Yb concentration, if there are no changes in the valence of the Ce or Yb ions that would modify their ionic radii or changes in bonding due to variation in the electron concentration. However, both lattice parameters remain roughly constant as  $x$  changes, indicating that the Ce and Yb ions do not retain the valences of the end member compounds ( $v_{Ce} = 3+$  for  $x = 0$  and  $v_{Yb} = 2+$  for  $x = 1$ ).

The EDX data reveal that crystals with the expected Yb concentration form for  $x < 0.8$ . For larger values of  $x$ , each peak in the XRD profile splits into two peaks [see the inset in Fig. 1(b)]: one with low intensity corresponding to the lattice constants for  $x < 0.8$  and a second one corresponding to the value expected for pure  $YbCoIn_5$ . The ratio of the integrated intensities for one pair of peaks is  $\sim 0.49$  for the case of  $x = 0.8$ , indicating phase separation into a minority phase (32%) and a majority phase (68%) that exhibit distinct Yb concentrations, where the latter is the Yb rich phase. The phase separation is further supported by the results of the EDX measurements (shaded region in Fig. 1). Similar results were recently reported by Capan *et al.* [16].

Electrical resistivity ( $\rho$ ) measurements were performed by using a standard four-wire technique. The shapes of the normalized electrical resistivity  $\rho/\rho(300\text{ K})$  curves (Fig. 2) for all samples with  $x \leq 0.775$  are typical of many HF materials; i.e., the data exhibit a weak  $T$  dependence at high  $T$  and a maximum or broad hump at  $T_{coh}$  that is followed by a decrease in  $\rho$  with decreasing  $T$ .

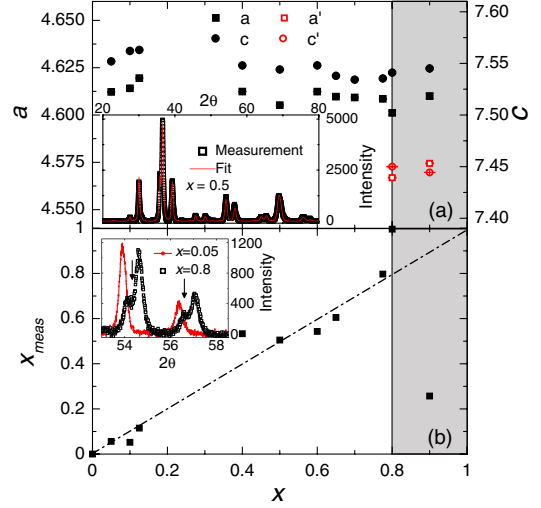


FIG. 1 (color online). (a) Lattice parameters  $a$  (filled black squares) and  $c$  (filled black circles) vs Yb concentration  $x$  for  $Ce_{1-x}Yb_xCoIn_5$ . Phase separation occurs for  $x \geq 0.8$ , and two sets of lattice constants are observed, as shown by the red open symbols that correspond to the lattice constants expected for  $YbCoIn_5$ . Inset: Representative XRD profile and Rietveld fit for  $x = 0.5$ . (b) Measured Yb concentration  $x_{meas}$  from EDX vs nominal  $x$ . Inset: Comparison of the XRD profiles for  $x = 0.05$  and  $0.8$ , illustrating the phase separation. The arrows highlight the splitting of the Bragg reflections (see the text).

This behavior is interpreted as the onset of coherent Kondo-like screening of the magnetic sublattice by the conduction electrons at  $T_{coh}$ . As the Yb concentration is increased,  $T_{coh}$  may be weakly suppressed initially, after which it remains roughly constant [Fig. 3(a)]. In contrast,  $YbCoIn_5$  does not exhibit correlated electron effects, suggesting an abrupt change in the behavior of the  $R$  sublattice between  $0 \leq x \leq 0.775$  and  $x = 1$ .

The normal-state  $\rho(T)$  data between  $T_c$  and  $\sim 25$  K for each substitution ( $x \leq 0.775$ ) can be fit with a power law  $\rho(T) = \rho_0 + AT^{n_\rho}$  [Fig. 2(b)]. A sub- $T$ -linear transport scattering rate (indicative of NFL behavior) is observed [12], which reaches a minimum value of  $n_\rho$  near  $x = 0.4$ ,

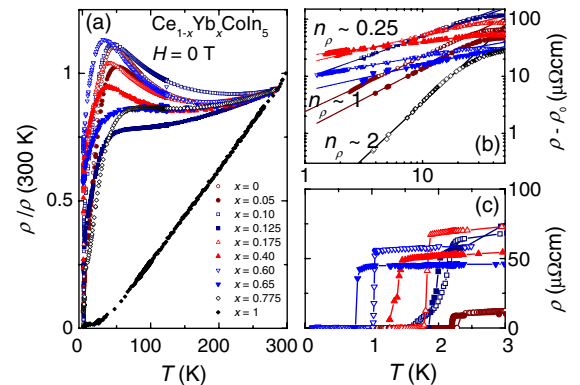


FIG. 2 (color online). (a) Electrical resistivity  $\rho$  normalized to its value at 300 K,  $\rho/\rho(300\text{ K})$ , vs temperature  $T$  for  $Ce_{1-x}Yb_xCoIn_5$  with  $0 \leq x \leq 1.0$ . (b) Power law fits for  $T_c < T < \sim 25$ . (c) Low  $T$  resistive superconducting transition curves.

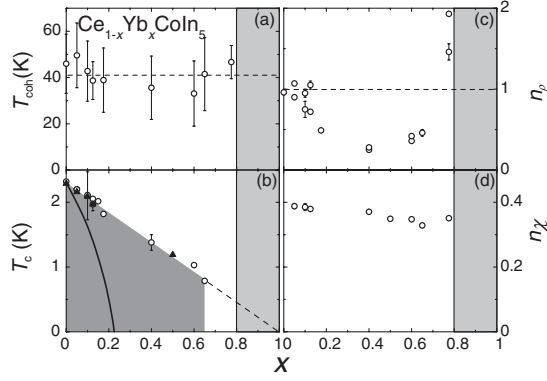


FIG. 3. (a) Coherence temperature  $T_{\text{coh}}$ , where  $\rho(T)$  exhibits a maximum (or knee) vs  $x$ . The error bars represent the width of the maximum, defined as the  $T$   $\rho = 0.95\rho_{\text{coh}}$ . (b) Circles:  $T_c$  determined from  $\rho(T)$  measurements vs  $x$  for  $\text{Ce}_{1-x}\text{Yb}_x\text{CoIn}_5$ . The vertical bars correspond to the 90% and 10% values of the superconducting transitions. Triangles:  $T_c$ , determined from  $C(T)$  measurements vs  $x$ . The solid line shows the suppression of  $T_c$  as reported for other rare earth substitutions [12]. (c) Fit parameters  $n_\rho$ , extracted from power law  $\rho = \rho_0 + AT^{n_\rho}$  fits to the normal-state resistivity vs  $x$ . (d) Fit parameters  $n_\chi$ , determined from fits of  $\chi_c = \chi_c(0) + a/T^{n_\chi}$  to the normal-state  $\chi(T)$  vs  $x$ . The light gray shading represents the region of phase separation.

after which it slowly recovers towards  $n_\rho \sim 2$  [Fig. 3(c)]. For  $x = 0.775$ , we find that  $A \approx 0.036 \mu\Omega \text{ cm}/\text{K}^2$ , implying that the ground state is a heavy Fermi liquid at this concentration. In order to explore this perspective, we have calculated the Kadowaki-Woods ratio  $R_{\text{KW}} = A/\gamma^2$ , which gives the relationship between the coefficient  $\gamma$  of the electronic specific heat and the coefficient  $A$  of the  $T^2$  contribution to the electrical resistivity, assuming that the system exhibits heavy FL behavior at low  $T$ . If we consider  $\gamma(2.3 \text{ K}) = 140 \text{ mJ/mol}\cdot\text{K}^2$  (Table I), then  $R_{\text{KW}} = 1.86 \times 10^{-6} \mu\Omega \text{ cm}(\text{mol}\cdot\text{K}/\text{mJ})^2$ . This value is intermediate between what is expected for Ce- and Yb-based heavy fermion compounds [17, 18], emphasizing that strong electronic correlations persist up to  $x \approx 0.775$ . SC transitions are clearly observed in  $\rho(T)$  for  $0 \leq x \leq 0.65$  [Fig. 2(c)], and there is a monotonic suppression of  $T_c$  with

TABLE I. Superconducting parameters for samples of  $\text{Ce}_{1-x}\text{Yb}_x\text{CoIn}_5$ . The values of  $T_c$  have been determined from specific heat data.  $\Delta C$  is the jump in  $C(T)$  at  $T_c$ , and  $\gamma(2.3 \text{ K})$  is the estimated electronic-specific-heat coefficient at 2.3 K.

$x$	$T_c$ (K)	$\Delta C$ (mJ/mol K)	$\gamma(2.3 \text{ K})$ (mJ/mol K <sup>2</sup> )
0	2.29	3460	357
0.05	2.16	3040	373
0.10	2.09	2240	347
0.125	1.97	1810	332
0.50	1.19	235	330
0.65			283
0.775			140

increasing Yb concentration [Fig. 3(b)]. In particular, we note that the  $T_c$  vs  $x$  curve extrapolates to 0 K near  $x = 1$ , emphasizing that the SC is anomalously robust in the presence of Yb substituents.

Magnetic susceptibility ( $\chi$ ) measurements were carried out as a function of  $T$  by using a Quantum Design SQUID magnetometer in  $H = 0.5 \text{ T}$ . Figures 4(a) and 4(b) show  $\chi(T)$  in the normal state for  $H$  applied in the  $ab$  plane,  $\chi_{ab}$ , and along the  $c$  axis,  $\chi_c$ . The ratio of  $\chi_{ab}$  to  $\chi_c$  at  $T = 2.3 \text{ K}$  is  $\sim 0.5$  [inset in Fig. 4(a)]. Surprisingly,  $\chi(T)$  retains a  $T$  dependence that is nearly identical to that of  $x = 0$  for  $x \leq 0.775$ ; i.e., Curie-Weiss behavior is observed at high  $T$ , after which  $\chi(T)$  saturates below 50 K, consistent with the onset of Kondo-like demagnetization and the coherent behavior observed in  $\rho(T)$ . These results are contrary to what would be expected if the Yb ions were to enter the lattice in the nonmagnetic divalent state, in which case  $\chi(T)$  should scale with  $(1-x)$ . Finally,  $\chi(T)$  again increases upon cooling below 20 K, contrary to the behavior of ideal HF compounds which are expected to remain in a FL state with a nearly  $T$ -independent  $\chi$  as  $T$  approaches 0 K. This upturn appears to be an intrinsic effect and not due to magnetic impurities, since we find that  $M(H)$  curves at low  $T$  do not saturate up to 70 kOe [19]. Between 1.8 and  $\sim 20 \text{ K}$ ,  $\chi_c$  can be fit by the form  $\chi_c = \chi_c(0) + a/T^{n_\chi}$ , consistent with the NFL behavior observed in  $\rho(T)$  and  $C(T)$ . Figure 3(d) shows the parameters  $n_\chi$ .

The specific heat ( $C$ ) was measured for  $0.3 \text{ K} \leq T \leq 5 \text{ K}$  in a Quantum Design Physical Properties Measurement System semiadiabatic calorimeter using a heat-pulse technique. Figure 5 shows  $C/T$  vs  $T$  for several values of  $x$ . The electronic-specific-heat coefficient  $\gamma = C/T$ , estimated to be the value of  $C/T$  near 2.3 K (Table I), reveals a substantial mass renormalization ( $\gamma \propto m^*$ ) that persists up to  $x = 0.65$ , after which  $\gamma$  is suppressed. Additionally,  $C/T$  tends to increase with

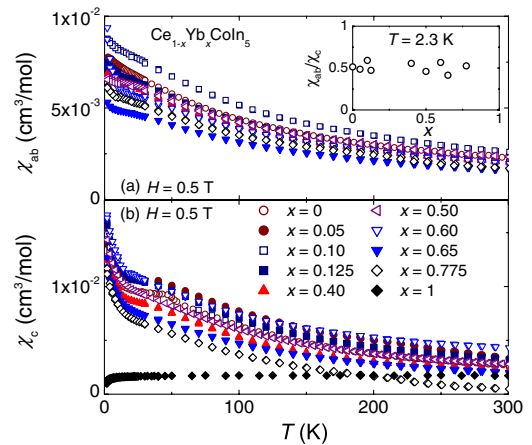


FIG. 4 (color online). (a) Magnetic susceptibility along the  $ab$  plane  $\chi_{ab}$  vs temperature  $T$  for  $\text{Ce}_{1-x}\text{Yb}_x\text{CoIn}_5$ . Inset: Ratio of  $\chi_{ab}$  to  $\chi_c$  at  $T = 2.3 \text{ K}$ . (b) Magnetic susceptibility along the  $c$  axis  $\chi_c$  vs  $T$  for  $\text{Ce}_{1-x}\text{Yb}_x\text{CoIn}_5$ . Data for  $x = 0$  are from Ref. [23].

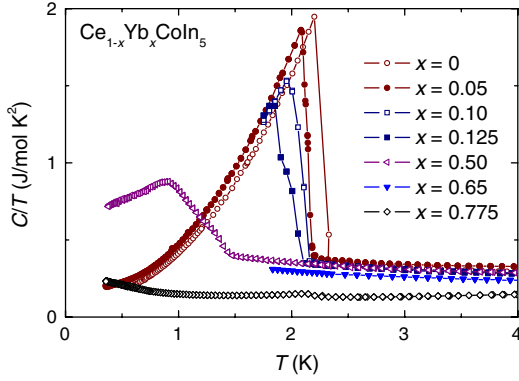


FIG. 5 (color online). Specific heat  $C$  divided by temperature  $T$  vs  $T$  for  $Ce_{1-x}Yb_xCoIn_5$ .

decreasing  $T$  down to the SC transition for all  $x$ , indicating that the low  $T$  NFL state persists up to  $x = 0.775$ .

For  $x \leq 0.125$ ,  $C(T)/T$  shows abrupt jumps at 2.1–2.3 K, while a broad transition is observed at low  $T$  for  $x = 0.5$ . From these data, we infer bulk SC for all  $x$ . We note that there is a very small feature in  $C/T$  for  $x = 0.775$  at  $T \sim 2.3$  K, which may be due to a SC transition arising from a  $CeCoIn_5$  impurity phase of 5%, as estimated from the size of the SC jump  $\Delta C$ . We note, however, that no additional peaks were observed in the XRD profiles for this concentration.

Our measurements demonstrate that  $Ce_{1-x}Yb_xCoIn_5$  exhibits an unconventional  $T$ - $x$  phase diagram without an apparent QCP, the Kondo-like lattice behavior and SC are preserved up to large values of  $x$ , and the NFL state is strongly modified with  $x$  (Fig. 3). These observations are striking, since previous studies of other  $Ce_{1-x}R_xCoIn_5$  systems have revealed that  $T_c$  and  $T_{coh}$  are rapidly and uniformly suppressed by both magnetic and nonmagnetic  $R$  ions, and, from a naive point of view, Yb substitution should yield similar results. Moreover,  $T_c$  does not scale with  $T_{coh}$ , as would be expected for a typical heavy fermion SC. Thus, it appears that Ce and Yb cooperatively change their electronic states in  $Ce_{1-x}Yb_xCoIn_5$  in such a way as to preserve the underlying Kondo-like lattice behavior and SC of  $CeCoIn_5$ . In contrast, the NFL state is strongly susceptible to the introduction of Yb ions, as observed for other  $R$  substituents in  $CeCoIn_5$ .

A possible explanation for this behavior can be found by considering VFs arising from a cooperative IV state formed by the Ce and Yb ions. In this scenario the substituted Yb ions “mimic” the electronic configuration of Ce, resulting in the anomalous preservation of the correlated electron state of the end member compound  $CeCoIn_5$  over a large range of  $x$  in  $Ce_{1-x}Yb_xCoIn_5$ . The cooperative IV state also provides a mechanism that may drive the observed NFL physics. It was recently suggested that quantum valence criticality yields NFL-like anomalies in the low  $T$  specific heat ( $C/T \sim -\ln T$ ), magnetic susceptibility ( $\chi \sim T^{-n_x}$ ,  $n_x = 0.5$ – $0.6$ ), and electrical resistivity

( $\Delta\rho \sim T$ ) as observed in other Yb-based compounds such as  $\beta$ - $YbAlB_4$  and  $YbRh_2(Si_{0.95}Ge_{0.05})_2$  [14,20,21]. We observe a  $T$ -linear and sub- $T$ -linear transport scattering rate in  $\rho$ , a weak inverse power law in  $\chi$ , and a low  $T$  increase of  $C/T$  in the normal state for  $Ce_{1-x}Yb_xCoIn_5$ . Moreover, QC VFs have been proposed to drive the NFL physics and unconventional SC in  $CeCu_2(Si_{1-x}Ge_x)_2$  [22].

In summary, the Kondo coherence and SC do not scale with the NFL behavior for  $Ce_{1-x}Yb_xCoIn_5$ , but ultimately these phenomena may be connected through cooperatively tuned IV states. In this scenario, NFL behavior and unconventional SC coexist over a large part of the phase diagram, in contrast with what is expected for classical QCP systems for which the NFL behavior and unconventional SC are tightly confined to a “V-shaped” region around the QCP. We conclude that  $Ce_{1-x}Yb_xCoIn_5$  belongs to a growing class of systems in which the NFL behavior occurs in the absence of an obvious QCP [4]. These results also suggest that VFs may play a role in the unconventional SC and NFL behavior in pure  $CeCoIn_5$ .

Crystal growth and characterization were funded by the U.S. DOE under Grant No. DE FG02-04ER46105. Low-temperature measurements were funded by the NSF under Grant No. 0802478. M.J. acknowledges financial support by the Alexander von Humboldt foundation.

\*Corresponding author.

mbmaple@ucsd.edu

- [1] C. M. Varma, Z. Nussinov, and W. v. Saarloos, *Phys. Rep.* **361**, 267 (2002).
- [2] N. D. Mathur *et al.*, *Nature (London)* **394**, 39 (1998).
- [3] H. v. Löhneysen, *J. Phys. Condens. Matter* **8**, 9689 (1996).
- [4] M. B. Maple *et al.*, *J. Low Temp. Phys.* **161**, 4 (2010).
- [5] V. A. Sidorov *et al.*, *Phys. Rev. Lett.* **89**, 157004 (2002).
- [6] J. R. Jeffries *et al.*, *Phys. Rev. B* **72**, 024551 (2005).
- [7] J. Paglione *et al.*, *Phys. Rev. Lett.* **91**, 246405 (2003).
- [8] A. D. Bianchi *et al.*, *Phys. Rev. Lett.* **91**, 257001 (2003).
- [9] A. D. Bianchi *et al.*, *Phys. Rev. Lett.* **89**, 137002 (2002).
- [10] A. D. Bianchi *et al.*, *Phys. Rev. Lett.* **91**, 187004 (2003).
- [11] H. A. Radovan *et al.*, *Nature (London)* **425**, 51 (2003).
- [12] J. Paglione *et al.*, *Nature Phys.* **3**, 703 (2007).
- [13] Y.-F. Yang *et al.*, *Nature (London)* **454**, 611 (2008).
- [14] S. Watanabe and K. Miyake, *Phys. Rev. Lett.* **105**, 186403 (2010).
- [15] V. S. Zapf *et al.*, *Phys. Rev. B* **65**, 014506 (2001).
- [16] C. Capan *et al.*, *Europhys. Lett.* **92**, 47004 (2010).
- [17] K. Kadowaki and S. B. Woods, *Solid State Commun.* **58**, 507 (1986).
- [18] N. Tsujii, H. Kontani, and K. Yoshimura, *Phys. Rev. Lett.* **94**, 057201 (2005).
- [19] T. Tayama *et al.*, *Phys. Rev. B* **65**, 180504 (2002).
- [20] J. Custers *et al.*, *Nature (London)* **424**, 524 (2003).
- [21] S. Nakatsuji *et al.*, *Nature Phys.* **4**, 603 (2008).
- [22] H. Q. Yuan *et al.*, *Phys. Rev. Lett.* **96**, 047008 (2006).
- [23] C. Petrovic *et al.*, *J. Phys. Condens. Matter* **13**, L337 (2001).